

# Single and multiple vibrational resonance in a quintic oscillator with monostable potentials

S. Jeyakumari,<sup>1</sup> V. Chinnathambi,<sup>1</sup> S. Rajasekar,<sup>2</sup> and M. A. F. Sanjuan<sup>3</sup>

<sup>1</sup>*Department of Physics, Sri KGS Arts College, Srivaikuntam 628 619, Tamilnadu, India*

<sup>2</sup>*School of Physics, Bharathidasan University, Tiruchirapalli 620 024, Tamilnadu, India*

<sup>3</sup>*Departamento de Física, Universidad Rey Juan Carlos, Tulipán s/n, 28933 Móstoles, Madrid, Spain*

(Received 22 July 2009; published 20 October 2009)

We analyze the occurrence of vibrational resonance in a damped quintic oscillator with three cases of single well of the potential  $V(x) = \frac{1}{2}\omega_0^2 x^2 + \frac{1}{4}\beta x^4 + \frac{1}{6}\gamma x^6$  driven by both low-frequency force  $f \cos \omega t$  and high-frequency force  $g \cos \Omega t$  with  $\Omega \gg \omega$ . We restrict our analysis to the parametric choices (i)  $\omega_0^2, \beta, \gamma > 0$  (single well), (ii)  $\omega_0^2, \gamma > 0, \beta < 0, \beta^2 < 4\omega_0^2\gamma$  (single well), and (iii)  $\omega_0^2 > 0, \beta$  arbitrary,  $\gamma < 0$  (double-hump single well). From the approximate theoretical expression of response amplitude  $Q$  at the low-frequency  $\omega$  we determine the values of  $\omega$  and  $g$  (denoted as  $\omega_{VR}$  and  $g_{VR}$ ) at which vibrational resonance occurs. We show that for fixed values of the parameters of the system when  $\omega$  is varied either resonance does not occur or it occurs only once. When the amplitude  $g$  is varied for the case of the potential with the parametric choice (i) at most one resonance occur while for the other two choices (ii) and (iii) multiple resonance occur. Further,  $g_{VR}$  is found to be independent of the damping strength  $d$  while  $\omega_{VR}$  depends on  $d$ . The theoretical predictions are found to be in good agreement with the numerical result. We illustrate that the vibrational resonance can be characterized in terms of width of the orbit also.

DOI: [10.1103/PhysRevE.80.046608](https://doi.org/10.1103/PhysRevE.80.046608)

PACS number(s): 46.40.Ff, 05.45.-a, 05.90.+m

## I. INTRODUCTION

The study of the influence of two-frequency signals is important in various branches of science and communication technologies [1–7]. In recent years investigation of resonance dynamics due to a biharmonic external force with two different frequencies  $\omega$  and  $\Omega$  with  $\Omega \gg \omega$  has received much interest. For example, in a bistable system Landa and McClintock [8] have shown the occurrence of resonant behavior with respect to a low-frequency force caused by the high-frequency force and later Gitterman [9] proposed an analytical treatment for this resonance phenomenon. Blekhnman and Landa [10] found single and double resonances in a double-well Duffing oscillator when the amplitude or frequency of the high-frequency modulation is varied. Vibrational resonance in a noise-induced structure [11] and FitzHugh-Nagumo equation [12,13] and experimental evidence of it in the analog simulation of the overdamped Duffing oscillator [14] and in an optical system [15,16] have also been reported. A theoretical approach has been proposed to characterize vibrational resonance in the presence of additive noise [17]. A comparative study of vibrational resonance with stochastic resonance in a two-coupled overdamped oscillator [18,19] and an analytical treatment of vibrational resonance in a overdamped bistable oscillator [20] were also presented. In a diode laser and logistic map the high-frequency force was found to induce noise-free stochastic resonance in an intermittency region [21].

In the present work both theoretically and numerically we study the vibrational resonance in a quintic oscillator with three forms of a monostable potential. The equation of motion of the quintic oscillator driven by two periodic forces is given by

$$\ddot{x} + d\dot{x} + \omega_0^2 x + \beta x^3 + \gamma x^5 = f \cos \omega t + g \cos \Omega t, \quad (1)$$

where  $\Omega \gg \omega$  and the potential of the system in the absence of damping and external force is

$$V(x) = \frac{1}{2}\omega_0^2 x^2 + \frac{1}{4}\beta x^4 + \frac{1}{6}\gamma x^6. \quad (2)$$

The shape of the potential  $V(x)$  depends on the sign of the three parameters  $\omega_0^2, \beta$ , and  $\gamma$ . It can be a single well, double well, triple well, single well with double hump, double well with double hump, and an inverted single well. The potential  $V(x)$  is used to model optical bistability in a dispersive medium where the refractive index is dependent on the optical intensity [22]. A triple-well case of the above potential is found to improve image sharpening in the presence of noise [23] and is also used to represent partially folded intermediates in proteins [24]. Such intermediates can accelerate the protein folding. Equation (1) in the absence of external periodic forces models a magnetoelastic beam in the nonuniform field of permanent magnets [25]. In recent years, various nonlinear phenomena have been studied in the quintic oscillator [26–34].

Here, we analyze the occurrence of vibrational resonance in system (1) with specific emphasize with single-well forms of the potential  $V(x)$ . We consider the parametric choices (i)  $\omega_0^2, \beta, \gamma > 0$  (single well) [Fig. 1(a)], (ii)  $\omega_0^2, \gamma > 0, \beta < 0, \beta^2 < 4\omega_0^2\gamma$  (single well) [Fig. 1(b)], and (iii)  $\omega_0^2 > 0, \beta$  arbitrary,  $\gamma < 0$  (double-hump single well) [Fig. 1(c)]. The reason for our interest in single-well cases of this system is that vibrational resonance is generally studied in bistable and multistable systems where for certain parametric choices multiple resonance is found. In the present work we analyze the possibility of multiple vibrational resonance in the single-well cases of system (1).

For  $\Omega \gg \omega$  the solution of system (1) consists of slow motion  $X(t)$  with frequency  $\omega$  and fast motion  $\psi(t, \Omega t)$  with frequency  $\Omega$ . For  $f \ll 1$  it is reasonable to assume that the amplitude of the slow oscillation is small so that nonlinear terms in the equation of motion of  $X$  can be neglected. This leads to an approximate analytical expression for the ampli-

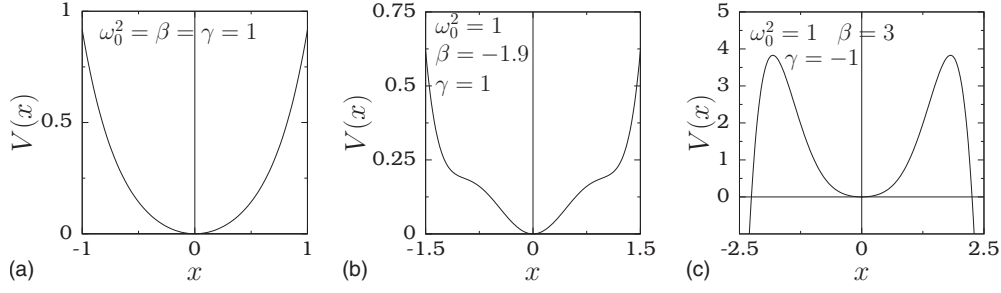


FIG. 1. Shape of the potential  $V(x)$  for (a)  $\omega_0^2, \beta, \gamma > 0$  (single well), (b)  $\omega_0^2, \gamma > 0, \beta < 0, \beta^2 < 4\omega_0^2\gamma$  (single well) and (c)  $\omega_0^2 > 0, \beta$ -arbitrary,  $\gamma < 0$  (double-hump single well).

tude (denoted as  $A_L$ ) of slow motion. The ratio of  $A_L$  and  $f$  is termed as response amplitude  $Q$ . Using this theoretical expression of  $Q$  we analyze the occurrence of vibrational resonance in system (1). For all the single-well forms of the potential we show that at most one resonance occur when the parameter  $\omega$  is varied. When  $g$  is varied we find that for the parametric choice (i) resonance occur at most once whereas multiple resonance occur for the parametric choices (ii) and (iii). The number of resonances, the values of  $\omega$  and  $g$  at which resonance occur (denoted as  $\omega_{VR}$  and  $g_{VR}$ ), are determined from the theoretical expression of  $Q$ . All the theoretical predictions are found to be in good agreement with the numerical calculation.

## II. THEORETICAL DESCRIPTION OF VIBRATIONAL RESONANCE

An approximate solution of Eq. (1) for  $\Omega \gg \omega$  can be obtained by the method of separation where solution is written as a sum of slow motion  $X(t)$  and fast motion  $\psi(t, \Omega t)$ :

$$x(t) = X(t) + \psi(t, \Omega t). \quad (3)$$

We assume that  $\psi$  is a periodic function with period  $2\pi/\Omega$  or  $2\pi$ -periodic function of fast time  $\tau = \Omega t$  and its mean value with respect to the time  $\tau$  is given by

$$\bar{\psi} = \frac{1}{2\pi} \int_0^{2\pi} \psi d\tau = 0. \quad (4)$$

Substituting the solution Eq. (3) into Eq. (1) and using Eq. (4), we obtain the following equations of motion for  $X$  and  $\psi$ :

$$\ddot{X} + d\dot{X} + (\omega_0^2 + 3\beta\bar{\psi}^2 + 5\gamma\bar{\psi}^4)X + (\beta + 10\gamma\bar{\psi}^2)X^3 + \gamma X^5 + \beta\bar{\psi}^3 + \gamma\bar{\psi}^5 = f \cos \omega t, \quad (5)$$

$$\begin{aligned} \ddot{\psi} + d\dot{\psi} + \omega_0^2\psi + 3\beta X^2(\psi - \bar{\psi}) + 3\beta X(\psi^2 - \bar{\psi}^2) + \beta(\psi^3 - \bar{\psi}^3) \\ + 5\gamma X^4(\psi - \bar{\psi}) + 10\gamma X^3(\psi^2 - \bar{\psi}^2) + 10\gamma X^2(\psi^3 - \bar{\psi}^3) \\ + 5\gamma X(\psi^4 - \bar{\psi}^4) + \gamma(\psi^5 - \bar{\psi}^5) + 10\gamma X^2\bar{\psi}^3 = g \cos \Omega t. \end{aligned} \quad (6)$$

Because  $\psi$  is a fast motion we assume that  $\ddot{\psi} \gg \dot{\psi}$ ,  $\psi$ ,  $\psi^2$ ,  $\psi^3$ ,  $\psi^4$ ,  $\psi^5$  and neglect all the terms in the left-hand side of Eq. (6) except the term  $\ddot{\psi}$ . This approximation called inertial ap-

proximation leads to the equation  $\ddot{\psi} = g \cos \Omega t$  the solution of which is given by

$$\psi = -\frac{g}{\Omega^2} \cos \Omega t. \quad (7)$$

For the  $\psi$  given by Eq. (7) we find

$$\bar{\psi}^2 = \frac{g^2}{2\Omega^4}, \quad \bar{\psi}^3 = 0, \quad \bar{\psi}^4 = \frac{3g^4}{8\Omega^4}, \quad \bar{\psi}^5 = 0. \quad (8)$$

Then Eq. (5) for the slow motion becomes

$$\ddot{X} + d\dot{X} + C_1 X + C_2 X^3 + \gamma X^5 = f \cos \omega t, \quad (9a)$$

where

$$C_1 = \omega_0^2 + \frac{3\beta g^2}{2\Omega^4} + \frac{15\gamma g^4}{8\Omega^8}, \quad C_2 = \beta + \frac{5\gamma g^2}{\Omega^4}. \quad (9b)$$

The effective potential corresponding to the slow motion of the system described by Eq. (8) is

$$V_{\text{eff}}(X) = \frac{1}{2} C_1 X^2 + \frac{1}{4} C_2 X^4 + \frac{1}{6} \gamma X^6. \quad (10)$$

The shape, the number of local maxima and minima and their location of the potential  $V(x)$  [Eq. (2)] depend on the parameters  $\omega_0^2$ ,  $\beta$ , and  $\gamma$ . For the effective potential ( $V_{\text{eff}}$ ) these depend also on the parameters  $g$  and  $\Omega$ . Consequently, by varying  $g$  or  $\Omega$  new equilibrium states can be created or the number of equilibrium states can be reduced.

The equilibrium points about which slow oscillations take place can be calculated from Eq. (8). The equilibrium points of Eq. (8) are given by

$$\begin{aligned} X_1^* = 0, \quad X_{2,3}^* = \pm \left[ \frac{-C_2 + \sqrt{C_2^2 - 4C_1\gamma}}{2\gamma} \right]^{1/2}, \\ X_{4,5}^* = \pm \left[ \frac{-C_2 - \sqrt{C_2^2 - 4C_1\gamma}}{2\gamma} \right]^{1/2}. \end{aligned} \quad (11)$$

Suppose, we choose  $\gamma > 0$ . Then we have the following cases:

Case (i):  $C_1, C_2 > 0$  or  $C_1 > 0, C_2 < 0$  with  $C_2^2 < 4C_1\gamma$ .  $X_1^* = 0$  is the only equilibrium point.

Case (ii):  $C_1 < 0, C_2$  arbitrary. There are three equilibrium points and are  $X_1^*, X_{2,3}^*$ .

Case (iii):  $C_1 > 0$ ,  $C_2 < 0$  with  $C_2^2 > 4C_1\gamma$ . There are five equilibrium points given by Eq. (11).

We obtain the equation for the deviation of the slow motion  $X$  from an equilibrium point  $X^*$ . Introducing the change in variable  $Y = X - X^*$  in Eq. (8) we get

$$\ddot{Y} + d\dot{Y} + \alpha_1 Y + \alpha_2 Y^2 + \alpha_3 Y^3 + \alpha_4 Y^4 + \gamma Y^5 = f \cos \omega t, \quad (12a)$$

where

$$\alpha_1 = C_1 + 3C_2 X^{*2} + 5\gamma X^{*4}, \quad (12b)$$

$$\alpha_2 = 3C_2 X^* + 10\gamma X^{*3}, \quad (12c)$$

$$\alpha_3 = C_2 + 10\gamma X^{*2}, \quad \alpha_4 = 5\gamma X^*. \quad (12d)$$

For  $f \ll 1$  and in the limit  $t \rightarrow \infty$  we assume that  $|Y| \ll 1$  and neglect the nonlinear terms in Eq. (11). Then, the solution of linear version of Eq. (11) in the limit  $t \rightarrow \infty$  is  $A_L \cos(\omega t - \phi)$ , where

$$A_L = \frac{f}{[(\omega_r^2 - \omega^2)^2 + d^2 \omega^2]^{1/2}}, \quad \phi = \tan^{-1} \left( \frac{\omega^2 - \alpha_1}{d\omega} \right), \quad (13)$$

and the resonant frequency is  $\omega_r = \sqrt{\alpha_1}$ . When the slow motion takes place around the equilibrium point  $X^* = 0$ , then  $\omega_r = \sqrt{C_1}$ .

The response amplitude  $Q$  is

$$Q = \frac{A_L}{f} = \frac{1}{[(\omega_r^2 - \omega^2)^2 + d^2 \omega^2]^{1/2}}. \quad (14)$$

In the following sections, we consider system (1) with three single-well cases of the potential  $V(x)$  separately and analyze the vibrational resonance using Eq. (14) and verify the theoretical results numerically.

### III. RESONANCE WITH SINGLE-WELL POTENTIAL ( $\omega_0^2$ , $\beta$ , $\gamma > 0$ )

For  $\omega_0^2$ ,  $\beta$ ,  $\gamma > 0$ , and  $V(x)$  is a single-well potential [Fig. 1(a)] with a local minimum at  $x=0$ . The quantities  $C_1$  and  $C_2$  given by Eq. (8) are now positive. Therefore, the effective potential is always a single-well potential when  $g$  or  $\Omega$  is varied. The slow motion is around the equilibrium point  $X_1^* = 0$  and  $\omega_r = \sqrt{C_1}$ .

We fix the parameters as  $\omega_0^2 = \beta = \gamma = 1$ ,  $f = 0.05$ ,  $d = 0.3$ , and  $\Omega = 10$ . Figures 2(a) and 2(b) show  $Q$  versus  $\omega$  for  $g = 25, 100, 150$  and  $Q$  versus  $g$  for  $\omega = 0.5, 1.25, 2$  respectively. Continuous curves represent theoretical result obtained from Eq. (14). Painted circles represent numerically calculated  $Q$ . We have calculated numerically the sine and cosine components  $Q_S$  and  $Q_C$ , respectively, from the equations

$$Q_S = \frac{2}{nT} \int_0^{nT} x(t) \sin \omega t dt, \quad (15a)$$

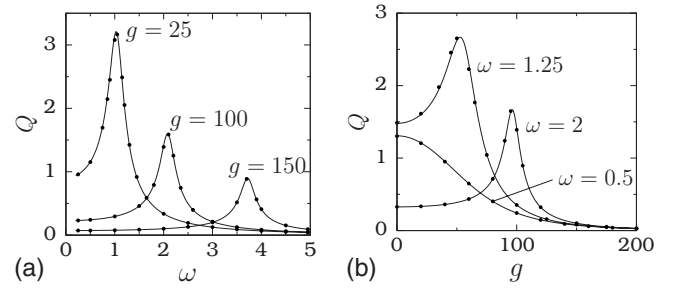


FIG. 2. (a) Response amplitude  $Q$  versus  $\omega$  for three values of  $g$ . (b)  $Q$  versus  $g$  for three values of  $\omega$ . Continuous curve represents theoretically calculated  $Q$  from Eq. (14) with  $\omega_r = \sqrt{C_1}$ , while painted circles represent numerically computed  $Q$  from Eqs. (15). The values of the other parameters are  $\omega_0^2 = \beta = \gamma = 1$ ,  $f = 0.05$ ,  $d = 0.3$ , and  $\Omega = 10$ .

$$Q_C = \frac{2}{nT} \int_0^{nT} x(t) \cos \omega t dt, \quad (15b)$$

where  $T = 2\pi/\omega$  and  $n$  is taken as 200. Then

$$Q = \frac{\sqrt{Q_S^2 + Q_C^2}}{f}. \quad (15c)$$

Numerically computed  $Q$  is in well agreement with the theoretical approximation. For  $g = 25, 100$ , and  $150$  the response amplitude  $Q$  is found to be maximum at  $\omega = 1.03, 2.08$ , and  $3.72$  respectively. In Fig. 2(b) for  $\omega = 0.5$  as  $g$  increases,  $Q$  decreases and resonance is not observed. For  $\omega = 1.25$  and  $\omega = 2$  resonance is found at  $g = 52.75$  and  $96.25$ , respectively. The above resonance phenomenon is termed as vibrational resonance as it is due to the presence of the high-frequency external periodic force.

The influence of resonance in  $X$  is seen in the width of the orbit of system (1). Figure 3(a) shows a phase portrait of system (1) for three values of  $g$ . The width of the orbit denoted as  $x_w$  is marked in this figure for the orbit corresponding to  $g = 52.75$ . In Fig. 3(b) we have plotted  $x_w$  against  $g$  for three values of  $\omega$ . This figure can be compared with Fig. 2(b). The variation in  $x_w$  is similar to the variation in  $Q$ .  $x_w$  is found to be maximum at resonance.



FIG. 3. Phase portrait of solution of Eq. (1) for three values of  $g$ . The inner orbit to the outer orbit the values of  $g$  are 10, 52.75, and 80, respectively.  $x_w$  denotes the width of the orbit for  $g = 52.75$ . (b) Variation in width of the orbit,  $x_w$ , as a function of  $g$  for three values of  $\omega$  corresponding to Fig. 2(b).

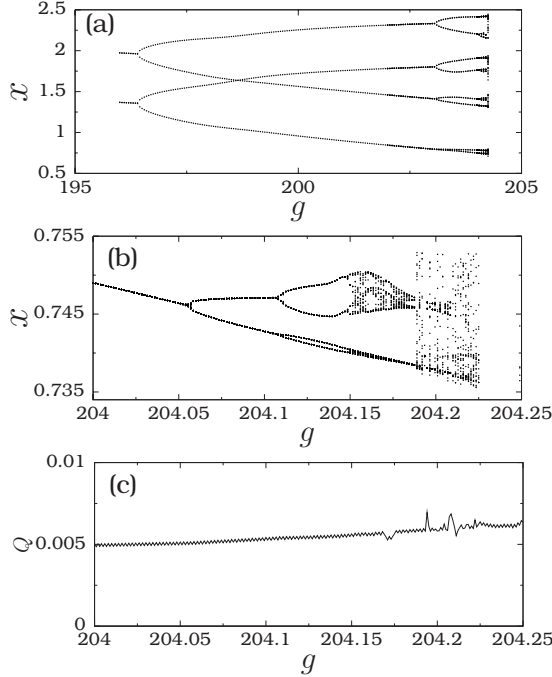


FIG. 4. (a) Bifurcation diagram showing period doubling phenomenon and chaotic dynamics. (b) Magnification of a small part of the bifurcation diagram. Numerically computed response amplitude corresponding to the subplot (b).

Since system (1) can exhibit variety of bifurcations of periodic orbits leading to chaotic motion and bifurcations of chaotic attractor, we examined the occurrence of them using bifurcation diagram and phase portrait. For certain cases of the parametric choices considered in our study chaotic motion is found for sufficiently large values of the control parameter  $g$ , particularly, far after resonance. An example is presented in Fig. 4(a) for  $\omega=2$ . For  $0 < g < 177.2$  a period- $T$  solution is found. When  $g$  is varied further period doubling phenomenon leading to chaotic motion, intermittency dynamics occur and are clearly seen in Fig. 4(b) which is a magnification of a small part of the bifurcation diagram Fig. 4(a). Onset of chaotic motion and sudden widening of a chaotic attractor occur at  $g=204.153$  and  $204.19$ , respectively. For  $g$  values just above  $204.2745$  period- $T$  solution is found. In Fig. 4(c) numerically calculated  $Q$  is plotted corresponding to Fig. 4(b). In the period doubling and chaotic regime  $Q \ll 1$ , that is, enhancement of amplitude of the signal at the low frequency not takes place.

The possibility of occurrence of resonance when a control parameter is varied and the values of a parameter at which resonance occurs can be determined from the theoretical expression of  $Q$ . The response amplitude  $Q$  given by Eq. (14) is a maximum when the function

$$S = (\omega_r^2 - \omega^2)^2 + d^2 \omega^2 \quad (16)$$

is a minimum. Thus, a local minimum of the function  $S$  represents a resonance. When a parameter, say,  $g$  is varied then resonance occurs at a value of  $g_{VR}$ , where  $g_{VR}$  is a root of the equation  $S_g = 4(\omega_r^2 - \omega^2)\omega_r\omega_{rg} = 0$  and  $S_{gg}|_{g=g_{VR}} = 8\omega\omega_{rg}^2 > 0$ .  $g_{VR}$  is obtained as

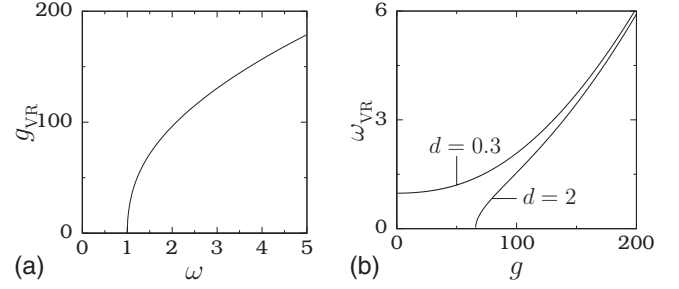


FIG. 5. Plots of (a)  $g_{VR}$  versus  $\omega$  [Eq. (16)] and (b)  $\omega_{VR}$  versus  $g$  [Eq. (18)] for system (1) with single-well potential.  $g_{VR}$  is independent of  $d$ .

$$g_{VR} = \Omega^2 \left[ \frac{-b + \sqrt{b^2 - 4ac}}{2a} \right]^{1/2}, \quad (17a)$$

where

$$a = \frac{15}{8}\gamma, \quad b = \frac{3}{2}\beta, \quad c = \omega_0^2 - \omega^2, \quad \omega^2 > \omega_0^2. \quad (17b)$$

Equation (16) implies that for  $\omega < \omega_0^2$  there is no resonance and for each value of  $\omega > \omega_0^2$  resonance occur at only one value of  $g = g_{VR}$ . Figure 5(a) shows the plot of  $g_{VR}$  versus  $\omega$ .  $g_{VR}$  increases with increase in  $\omega > \omega_0^2 = 1$ .

For a fixed value of  $g$  we obtain

$$\omega_{VR} = \sqrt{\omega_r^2 - \frac{d^2}{2}}, \quad \omega_r^2 > \frac{d^2}{2}. \quad (18)$$

When  $\omega$  is varied from zero the resonant frequency remains constant because it is independent of  $\omega$ . Consequently, the function  $S$  will have at most one local minimum and hence resonance will occur at most one value of  $\omega$ . This is the case for other forms of the potential also. Multiple resonance is thus not possible when  $\omega$  is treated as a control parameter.  $g_{VR}$  given by Eq. (16) is independent of the damping strength  $d$ , while  $\omega_{VR}$  depends on  $d$ . Resonance will not occur for the parametric choices for which  $\omega_r^2 = C_1 < d^2/2$ . The requirement  $C_1 > d^2/2$  is not satisfied for  $g_- < g < g_+$ , where

$$g_{\pm} = \Omega^2 \left[ \frac{-b \pm \sqrt{b^2 - 4a(\omega_0^2 - \frac{d^2}{2})}}{2a} \right]^{1/2}. \quad (19)$$

For  $d^2 < 2\omega_0^2$  resonance occur at  $\omega_{VR}$  given by Eq. (18) for each fixed value of  $g$  while for  $d^2 > 2\omega_0^2$  resonance will occur only if  $g > g_+$ .  $g_+ = 65.78$  for  $\omega_0^2 = \beta = \gamma = 1$ ,  $d = 2$ , and  $\Omega = 10$ . Figure 5(b) shows  $\omega_{VR}$  versus  $g$  for  $d = 0.3$  and  $2$ .

#### IV. SINGLE-WELL POTENTIAL WITH $\omega_0^2, \gamma > 0, \beta < 0, \beta^2 < 4\omega_0^2\gamma$

In this section we consider the system (1) with the single-well potential of the form shown in Fig. 1(b) where  $\omega_0^2, \gamma > 0, \beta < 0, \beta^2 < 4\omega_0^2\gamma$ . In this case the sign of both  $C_1$  and  $C_2$  can be changed by varying either  $g$  or  $\Omega$ . The effective potential can change into other forms. Figure 6 depicts  $V_{\text{eff}}$  for three values of  $g$  where  $\omega_0^2 = 1, \beta = -1.9, \gamma = 1$ , and  $\Omega = 10$ .  $V_{\text{eff}}$  is a single-well potential for  $g = 70$  and  $100$  while it becomes a double-well potential for  $g = 90$ .

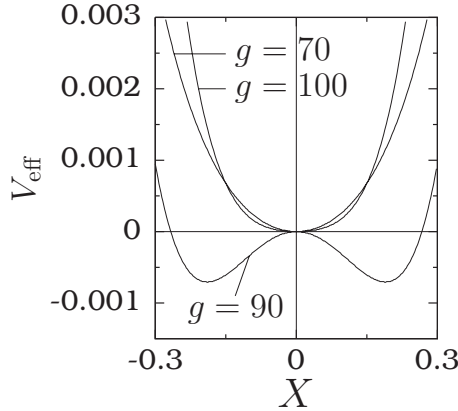


FIG. 6. Shape of the effective potential  $V_{\text{eff}}$  for  $\omega_0^2=1$ ,  $\beta=-1.9$ ,  $\gamma=1$ ,  $\Omega=10$  and for three values of  $g$ .

$\omega_{\text{VR}}$  is given by Eq. (18) where  $\omega_r^2=C_1$  if  $V_{\text{eff}}$  is a single-well form while  $\omega_r^2=\alpha_1$  for the double-well case. Figure 7 shows  $\omega_{\text{VR}}$  versus  $g$  for three values of  $d$ .  $\omega_{\text{VR}}$  is single valued. Above a certain critical value of  $d$  and for certain range of fixed values of  $g$  resonance cannot occur when  $\omega$  is varied. For example, for  $d=0.3$  resonance cannot be observed for  $g \in [70.62, 76.14]$  and  $[96.94, 101.06]$ . Analytical expression for the width of such nonresonance regime is difficult to obtain because  $\omega_r^2=\alpha_1$  is a complicated function of  $g$ . In Fig. 7 we notice that the nonresonance interval of  $g$  increases with  $d$ .

The values of  $g_{\text{VR}}$  when the effective potential is a single well are given by Eq. (16) for  $\omega^2 > \omega_0^2$ , whereas for  $\omega_0^2 - 3\beta^2/10\gamma < \omega^2 < \omega_0^2$

$$g_{\text{VR}} = \Omega^2 \left[ \frac{-b \pm \sqrt{b^2 - 4ac}}{2a} \right]^{1/2}. \quad (20)$$

When  $V_{\text{eff}}$  becomes a double well an analytical expression for  $g_{\text{VR}}$  is difficult to find. In this case  $g_{\text{VR}}$  can be calculated numerically. We determine the roots of  $S_g = 4(\omega_r^2 - \omega^2)\omega_r\omega_{rg} = 0$  and  $g_{\text{VR}}$  numerically by analyzing the cases  $\omega_r^2 - \omega^2 = 0$  and  $\omega_{rg} = 0$ . Figure 8(a) shows  $g_{\text{VR}}$  against  $\omega$ .  $g_{\text{VR}}=87.05$  for  $\omega > 0.412$  arises from  $\omega_{rg}=0$ . For  $\omega < 0.412$  resonance occurs at four values of  $g$ . Three resonances occur for  $0.412 < \omega < 1$ . For  $\omega > 1$  two resonances occur.  $V_{\text{eff}}$  is a single well for  $0 < g < 74.14$  (region I), double well for  $74.14 < g < 98.5$  (region II) and again become a single well for  $g > 98.5$  (region III). In the region I a resonance takes place

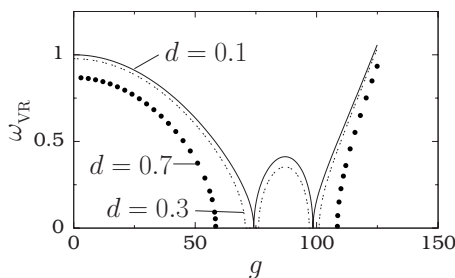


FIG. 7. Plot of  $\omega_{\text{VR}}$  versus  $g$  for three fixed values of  $d$  with  $\omega_0^2=1$ ,  $\beta=-1.9$ ,  $\gamma=1$ , and  $\Omega=10$ .

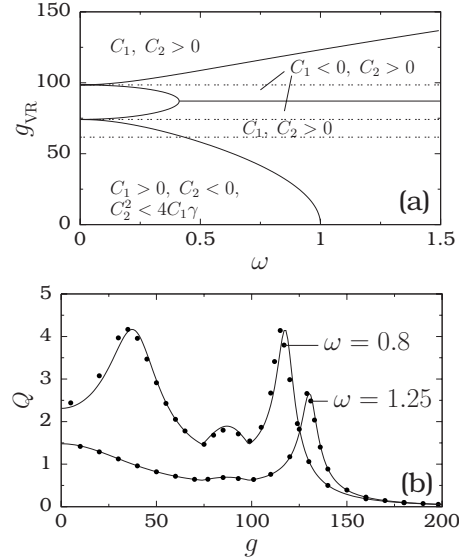


FIG. 8. (a)  $g_{\text{VR}}$  versus  $\omega$  with  $\omega_0^2=1$ ,  $\beta=-1.9$ ,  $\gamma=1$ , and  $\Omega=10$ . The effective potential is a single well for  $0 < g < 61.65$  where  $C_1 > 0$ ,  $C_2 < 0$ ,  $C_2^2 < 4C_1\gamma$ , and  $61.65 < g < 74.14$  where  $C_1, C_2 > 0$ ; double well for  $74.14 < g < 98.5$ , where  $C_1 < 0$ ,  $C_2 > 0$  and again a single well for  $g > 98.5$  where  $C_1, C_2 > 0$ . (b)  $Q$  versus  $g$  for two values of  $\omega$  where  $\Omega=10$ ,  $d=0.3$ , and  $f=0.05$ . Continuous curves are theoretical result while the painted circles are numerically computed values of  $Q$ .

only if  $\omega^2 < \omega_0^2 (=1)$ ; in the region II resonance occurs at two values of  $g$  for  $\omega < 0.412$ , while one resonance takes place at  $g_{\text{VR}}=87.05$  for  $\omega > 0.412$ ; in the region III single resonance occurs. The resonance curves in the regions I and III for  $\omega^2 < \omega_0^2$  are given by Eq. (20) while the curve in the region-III for  $\omega^2 > \omega_0^2$  is given by Eq. (16). The resonance curve in the region II corresponds to double-well case of  $V_{\text{eff}}$ . In Fig. 8(b) we can clearly see the resonance at three values of  $g$  for  $\omega=0.8$ . The value of  $Q$  at  $g_{\text{VR}}=87.05$  is much smaller than the values of other  $g_{\text{VR}}$ . The value of  $Q$  decreases when  $\omega$  increases.

In the single-well system (1) with  $\omega_0^2=1$ ,  $\beta=-1.9$ ,  $\gamma=1$  when  $g$  is varied from 0 the effective potential underwent transitions from single well to a double well and then to a single well and multiple resonance is found. In the next section, we show an example of multiple resonance where the form of the effective potential remains as a double-hump single well.

### V. DOUBLE-HUMP SINGLE-WELL POTENTIAL WITH $\omega_0^2 > 0$ , $\beta$ -ARBITRARY, $\gamma < 0$

$V(x)$  is a single-well double-hump potential [Fig. 1(c)] for  $\omega_0^2 > 0$ ,  $\beta$ -arbitrary,  $\gamma < 0$  with a local minimum at  $x=0$  and two local maxima at  $x = \pm [-\beta - \sqrt{\beta^2 - 4\omega_0^2\gamma}]/(2\gamma)$ . We assume that  $\beta > 0$  and fix  $\omega_0^2=1$ ,  $\beta=3$ ,  $\gamma=-1$ , and  $\Omega=10$ . For  $0 < g < 78.55$   $V_{\text{eff}}$  is a single-well double-hump potential with  $C_1, C_2 > 0$ ; for  $78.55 < g < g_c=161.3925$  it is again of same form but with  $C_1 > 0$ ,  $C_2 < 0$ , and for  $g > g_c$  it is an inverted potential. That is, the shape of  $V_{\text{eff}}$  does not change into a double well or a triple well as  $g$  is varied from zero.

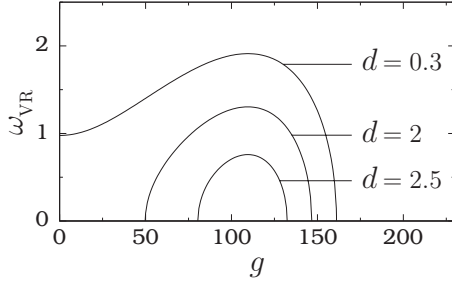


FIG. 9.  $\omega_{\text{VR}}$  versus  $g$  for three different values of  $d$  with  $\omega_0^2 = 1$ ,  $\beta = 3$ ,  $\gamma = -1$ , and  $\Omega = 10$ .

However, we notice multiple resonance when  $g$  is varied. For  $g < g_c$  the resonant frequency is  $\sqrt{C_1}$  and for  $g > g_c$  the motion of the system becomes unbound.

We consider the dependence of  $\omega_{\text{VR}}$  on  $g$ .  $\omega_{\text{VR}}$  is given by Eq. (18). From the requirement  $\omega_r^2 = C_1 > d^2/2$  we find that for  $d^2 > 2\omega_0^2$  when  $\omega$  is varied resonance will occur only if  $g_- < g < g_+$ , where

$$g_{\pm} = \Omega^2 \left[ \frac{b \pm \sqrt{b^2 + 4|a| \left( \omega_0^2 - \frac{d^2}{2} \right)}}{2|a|} \right]^{1/2}. \quad (21)$$

Examples for this are shown in Fig. 9 for  $d = 2$  and  $2.5$ . For  $d^2 < 2\omega_0^2$  resonance will occur for  $0 < g < g_+$  [see  $\omega_{\text{VR}}$  versus  $g$  for  $d = 0.3$  in Fig. 9]. The nonresonance intervals of  $g$  increases with increase in  $d$ . Figures 5(b), 7, and 9 can be compared.

Figure 10 shows plot of  $\omega_r$  versus  $g$  and  $\omega_{\text{rg}}$  versus  $g$ . In Fig. 10(a) as  $g$  increases from 0 the value of  $\omega_r$  increases from  $\omega_{r1} = 1$  reaches a maximum value  $\omega_{r2} = 1.924$  at  $g = g_0 = 109.54$  and then decreases and reaches again the value  $\omega_{r1}$  at  $g = g_1 = 155$ . This is because  $C_1$ , the square root of which is  $\omega_r$ , is a nonmonotonically varying function of  $g$ .

From Fig. 10 we infer the following:

(i) For  $0 < \omega < \omega_{r1}$  the quantity  $\omega_r^2 - \omega^2$  is zero for a value of  $g$  in the interval  $[g_1 = 155, g_c = 161.3925]$  and thus a resonance.

(ii) For each value of  $\omega$  in the interval  $[\omega_{r1}, \omega_{r2}]$ ,  $\omega_r^2 - \omega^2 = 0$  for two values of  $g$  in the interval  $[0, g_1]$  and hence two resonances—one for  $g < g_0$  and another for  $g_0 < g < g_1$ .

(iii)  $\omega_{\text{rg}} = 0$  at  $g = g_0$  with  $S_{g_0} = -36(\omega_{r2}^2 - \omega^2) / \omega_{r2}^2$ . There is only one resonance for  $\omega > \omega_{r2}$  and is at  $g = g_0$ .

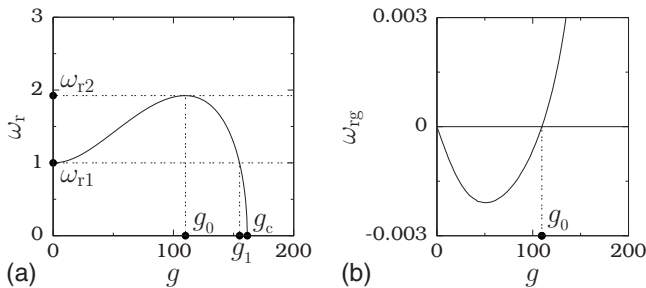


FIG. 10. (a)  $\omega_r$  versus  $g$  and (b)  $\omega_{\text{rg}}$  versus  $g$  for  $\omega_0^2 = 1$ ,  $\beta = 3$ ,  $\gamma = -1$ , and  $\Omega = 10$ .

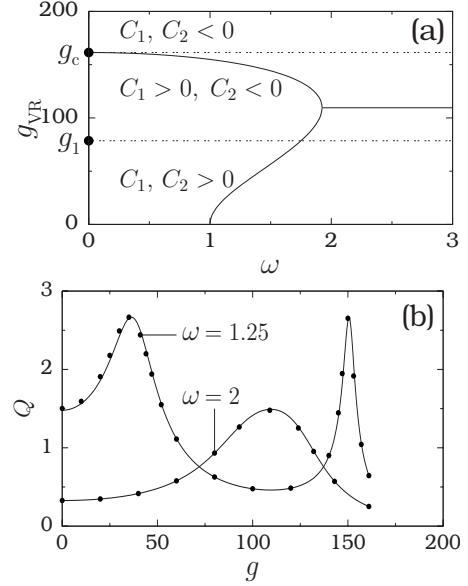


FIG. 11. (a)  $\omega$  versus  $g_{\text{VR}}$  for the system (1) with a double-hump single-well potential. Here  $\omega_0^2 = 1$ ,  $\beta = 3$ ,  $\gamma = -1$ , and  $\Omega = 10$ . The effective potential is a single-well double-hump form for  $0 < g < g_c = 161.3925$ , where  $C_1 > 0$  and  $C_2$  arbitrary and becomes an inverted single-well for  $g > g_c$ . (b) Response amplitude  $Q$  as a function  $g$  for two values of  $\omega$  where  $f = 0.05$  and  $d = 0.3$ . Continuous curves are theoretical result while the painted circles are numerically computed values of  $Q$ .

Interestingly, analytical expressions for  $g_{\text{VR}}$  due to  $\omega_{\text{rg}} = 0$  and  $\omega_r^2 - \omega^2 = 0$  can be obtained.  $\omega_{\text{rg}} = 0$  gives

$$g_{\text{VR}} = g_0 = \Omega^2 \sqrt{\frac{2\beta}{5|\gamma|}}, \quad \omega > \omega_r(g_0) = \omega_{r2}. \quad (22)$$

On the other hand,  $\omega_r^2 - \omega^2 = 0$  gives

$$g_{\text{VR}} = \Omega^2 \left[ \frac{b + \sqrt{b^2 + 4|a|(\omega_0^2 - \omega^2)}}{2|a|} \right]^{1/2}, \quad \omega^2 < \omega_0^2 \quad (23)$$

and

$$g_{\text{VR}} = \Omega^2 \left\{ \frac{b \pm \sqrt{b^2 - 4|a|(\omega_0^2 - \omega^2)}}{2|a|} \right\}^{1/2},$$

$$\omega_0^2 < \omega^2 < [\omega_r(g_0)]^2 = \omega_0^2 + \frac{3\beta^2}{10|\gamma|}, \quad (24)$$

where  $a$  and  $b$  are given by Eq. (16).

Figure 11(a) depicts  $\omega$  versus  $g_{\text{VR}}$ . Figure 11(b) shows the variation in  $Q$  versus  $g$  for two fixed values of  $\omega$  with  $d = 0.3$  and  $f = 0.05$ . In Fig. 11(b) we notice that  $Q$  at  $g = g_0$  is a minimum for  $\omega = 1.25$ , and it becomes a maximum for  $\omega = 2$ . For  $\omega = 1.25$  two resonances are observed at  $g = 36.5$  and  $150.6$ , while for  $\omega = 2$  resonance is found only at  $g = g_0$ . In the double-hump single-well system multiple resonance occurs because the resonant frequency  $\omega_r$  of the slow motion is a nonmonotonically varying function of  $g$ . Even though the effective potential not changes into a double-well or a triple-well form, as  $g$  increases from 0 the resonant frequency in-

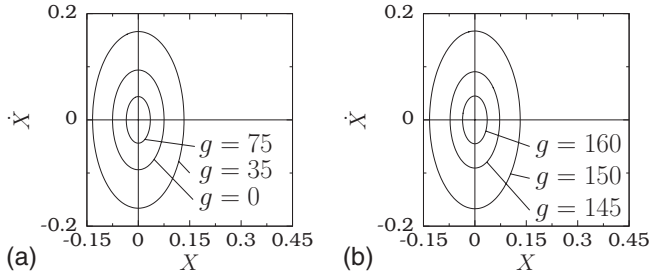


FIG. 12. Phase portrait of slow motion of system (1) with double-hump single-well potential for three values of  $g$  around the two resonances at  $g=36.5$  and  $150.6$  for  $\omega=1.25$ ,  $f=0.05$ ,  $\Omega=10$ , and  $d=0.3$ .

creases for a while and then decreases. Consequently, for a range of fixed values of  $\omega$ ,  $(\omega_r^2 - \omega^2)$  in Eq. (14) becomes minimum ( $=0$ ) at two values of  $g$ . Therefore, two resonances are observed when  $g$  is varied for certain range of fixed values of  $\omega$ . Figure 12 shows slow motion of the system around the two resonances for  $\omega=1.25$ . All the orbits oscillate about the origin.

In the case of Duffing oscillator with the potential  $V(x) = \frac{1}{2}\omega_0^2 x^2 + \frac{1}{4}\beta x^4$  occurrence of multiple resonance is not possible when  $V$  is a single-well or a double-hump single-well form as shown below. We have

$$V_{\text{eff}}(X) = \frac{1}{2}C_1 X^2 + \frac{1}{4}C_2 X^4, \quad C_1 = \omega_0^2 + \frac{3\beta g^2}{2\Omega^4}, \quad C_2 = \beta. \quad (25)$$

$V(x)$  is a single-well potential for  $\omega_0^2, \beta > 0$ , double-well potential for  $\omega_0^2 < 0, \beta > 0$ , single-well double-hump potential for  $\omega_0^2 > 0, \beta < 0$ , and an inverted single-well potential for  $\omega_0^2, \beta < 0$ . For the single-well case the values of  $C_1$  and  $C_2$  are always  $> 0$  and the effective potential remains a single well. The resonant frequency  $\omega_r = \sqrt{C_1}$  increases continuously from  $\omega_0$  as  $g$  increases from 0 and

$$g_{\text{VR}} = \Omega^2 \sqrt{\frac{2(\omega^2 - \omega_0^2)}{3\beta}}. \quad (26)$$

Hence, as  $g$  increases from 0, resonance does not occur for  $\omega^2 < \omega_0^2$  and only one resonance occurs for  $\omega^2 > \omega_0^2$  at  $g = g_{\text{VR}}$  given by Eq. (26).

For the single-well double-hump potential we have  $C_2 < 0$  (always) and  $C_1 = \omega_0^2 - 3|\beta|g^2/(2\Omega^4)$ . At  $g=0$ ,  $\omega_r = \sqrt{C_1} = \omega_0$ . As  $g$  increases from 0,  $\omega_r$  decreases monotonically from  $\omega_0$  and becomes 0 at  $g = g_1 = \Omega^2 \sqrt{2\omega_0^2/(3|\beta|)}$ . Thus, for  $\omega^2 < \omega_0^2$  there is a resonance at a value of  $g$  given by Eq. (26). (For  $\omega^2 > \omega_0^2$  resonance does not occur.) When  $g$  is further increased from  $g_1$  the effective potential becomes an

inverted single-well form and the motion of the system is unbounded. Thus, at most one resonance occur in the Duffing oscillator with the single-well double-hump potential. Whereas in the expression for  $C_1$  in  $V_{\text{eff}}$  of the quintic oscillator there are two terms depending on  $g$  and the sign of these two terms are different. The result is  $\omega_r^2 = C_1$  oscillates over a certain range of  $g$  (or  $\Omega$ ).

## VI. CONCLUSION

For the quintic oscillator, from the analysis of the approximate theoretical expression of response amplitude  $Q$  of slow motion, we are able to determine the number of resonances and the values of the control parameter, say,  $g$  or  $\omega$  or  $\Omega$ , at which resonance occur. Irrespective of whether the quintic oscillator potential  $V$  has a single well or a multiwell, as  $\omega$  varies either no resonance or only one resonance occur (when  $\omega^2 - \omega_r^2 + d^2/2 = 0$ ) depending upon the values of other parameters. As  $g$  is varied we have the following results: (i) resonance occur when either  $\omega_r^2 - \omega^2 = 0$  or  $\omega_{rg} = 0$  with  $S_{gg} > 0$ . (ii) In the single-well case with  $\omega_0^2, \beta, \gamma > 0$  the resonant frequency  $\omega_r$  increases monotonically from  $\omega_0$  and hence only one resonance occur for  $\omega^2 > \omega_0^2$  at the value of  $g$  given by Eq. (16). (iii) In the case of single-well with  $\omega_0^2, \gamma > 0, \beta < 0, \beta^2 < 4\omega_0^2\gamma$  the effective potential changes from single well to double well and then to single well for a range of fixed values of  $\omega$ .  $\omega_r$  oscillates over a range of  $g$  such that  $\omega_r^2 - \omega^2 = 0$  is realized at more than one value of  $g$  leading to a multiple resonance. (iv) When the potential of the system is a single-well double-hump potential, double resonance is noticed in the interval of  $g$  where the effective potential remains as the single-well double-hump shape, however,  $\omega_r$  is found to oscillate.

Our analysis indicates that to observe resonance bistability and transition of  $V_{\text{eff}}$  from one form to another form are not necessary. A monostable system can be able to exhibit multiple vibrational resonance if the resonant frequency  $\omega_r$  oscillates. Further, not only the case  $\omega_r^2 - \omega^2 = 0$  but also the case  $\omega_{rg} = 0$  with  $S_{gg} > 0$  corresponds to a resonance.

We have shown that the presence of resonance can be identified using the width of the orbit  $x_w$ . The numerical calculation of  $x_w$  is much easier than the numerical calculation of  $Q$ . Analysis of vibrational resonance in nonlinearly damped system and parametrically driven system can provide further insight on the occurrence of vibrational resonance.

## ACKNOWLEDGMENTS

The work of S.R. forms part of a Department of Science and Technology, Government of India sponsored research project. M.A.F.S. acknowledges financial support from the Spanish Ministry of Education and Science under Project No. FIS2006-08525.

- [1] V. Mironov and V. Sokolov, *Radiotekh. Elektron. (Moscow)* **41**, 1501 (1996).
- [2] D. Su, M. Chiu, and C. Chen, *Precis. Eng.* **18**, 161 (1996).
- [3] A. Maksimov, *Ultrasonics* **35**, 79 (1997).
- [4] A. Gherm, N. Zernov, B. Lundborg, and A. Vastberg, *J. Atmos. Sol.-Terr. Phys.* **59**, 1831 (1997).
- [5] A. D. Phelps, G. G. Ramble, and T. G. Leighton, *J. Acoust. Soc. Am.* **101**, 1981 (1997).
- [6] J. Victor and M. Conte, *Visual Neurosci.* **17**, 959 (2000).
- [7] M. M. Mahmoodian, L. S. Braginsky, and M. V. Entin, *Phys. Rev. B* **74**, 125317 (2006).
- [8] P. S. Landa and P. V. E. McClintock, *J. Phys. A* **33**, L433 (2000).
- [9] M. Gitterman, *J. Phys. A* **34**, L355 (2001).
- [10] I. I. Blekhman and P. S. Landa, *Int. J. Non-Linear Mech.* **39**, 421 (2004).
- [11] A. A. Zaikin, L. Lopez, J. P. Baltanas, J. Kurths, and M. A. F. Sanjuan, *Phys. Rev. E* **66**, 011106 (2002).
- [12] E. Ullner, A. Zaikin, J. Garcia-Ojalvo, R. Bascones, and J. Kurths, *Phys. Lett. A* **312**, 348 (2003).
- [13] B. Deng, J. Wang, and X. Wei, *Chaos* **19**, 013117 (2009).
- [14] J. P. Baltanas, L. Lopez, I. I. Blechman, P. S. Landa, A. Zaikin, J. Kurths, and M. A. F. Sanjuan, *Phys. Rev. E* **67**, 066119 (2003).
- [15] V. N. Chizhevsky, E. Smeu, and G. Giacomelli, *Phys. Rev. Lett.* **91**, 220602 (2003).
- [16] V. N. Chizhevsky and G. Giacomelli, *Phys. Rev. E* **70**, 062101 (2004).
- [17] J. Casado-Pascual and J. P. Baltanas, *Phys. Rev. E* **69**, 046108 (2004).
- [18] V. M. Gandhimathi, S. Rajasekar, and J. Kurths, *Phys. Lett. A* **360**, 279 (2006).
- [19] V. M. Gandhimathi and S. Rajasekar, *Phys. Scr.* **76**, 693 (2007).
- [20] V. N. Chizhevsky, *Int. J. Bifurcation Chaos Appl. Sci. Eng.* **18**, 1767 (2008).
- [21] T. Jungling, H. Benner, T. Stemler, and W. Just, *Phys. Rev. E* **77**, 036216 (2008).
- [22] Y. H. Kao and C. S. Wang, *Phys. Rev. E* **48**, 2514 (1993).
- [23] G. Gilboa, N. Sochen, and Y. Y. Zeevi, *J. Math. Imaging Vision* **20**, 121 (2004).
- [24] C. Wagner and T. Kiefhaber, *Proc. Natl. Acad. Sci. U.S.A.* **96**, 6716 (1999).
- [25] G. Z. Li and F. C. Moon, *J. Sound Vib.* **136**, 17 (1990).
- [26] J. Yu, R. Zhang, W. Pan, and L. Schimansky-Geier, *Phys. Scr.* **78**, 025003 (2008).
- [27] R. Tchoukuegno, B. R. Nana Nbandjo, and P. Wofo, *Physica A* **304**, 362 (2002).
- [28] R. Tchoukuegno and P. Wofo, *Physica D* **167**, 86 (2002).
- [29] A. Yu. Kuznetsova, A. P. Kuznetsov, C. Knudsen, and E. Mosekilde, *Int. J. Bifurcation Chaos Appl. Sci. Eng.* **14**, 1241 (2004).
- [30] Z. Jing, Z. Yang, and T. Jiang, *Chaos, Solitons Fractals* **27**, 722 (2006).
- [31] M. Siewe, F. M. Moukam Kakmeni, C. Tchawoua, and P. Wofo, *Physica A* **357**, 383 (2005).
- [32] R. Tchoukuegno, B. R. Nana Nbandjo and P. Wofo, *Int. J. Non-Linear Mech.* **38**, 531 (2003).
- [33] F. So and K. Liu, *Physica A* **303**, 79 (2002).
- [34] P. K. Ghosh, B. C. Bag, and D. S. Ray, *Phys. Rev. E* **75**, 032101 (2007).